

Bound Ro-Vibronic States of Triplet H_3^+

Oliver Friedrich and Alexander Alijah*

Fakultät für Chemie, Universität Bielefeld, 33615 Bielefeld, Germany

ZongRong Xu and António J. C. Varandas*

Departamento de Química, Universidade de Coimbra, 3049 Coimbra Codex, Portugal

(Received 20 June 2000; revised manuscript received 10 October 2000)

On the basis of a new, highly accurate potential energy hypersurface for the lowest triplet state of H_3^+ , $^3\Sigma_u^+$, the bound ro-vibronic states are calculated for $J \leq 5$. Since the potential has very shallow minima, those states exist only up to single vibrational excitation. The symmetry properties of the ro-vibrational states are investigated. Further, it is demonstrated that the first excited triplet state, which intersects conically with the $^3\Sigma_u^+$ state, has no effect on the reported ro-vibrational energies.

DOI: 10.1103/PhysRevLett.86.1183

PACS numbers: 33.20.Vq, 03.65.Ge

I. Introduction.—Up to the present time the simplest triatomic molecule, H_3^+ , challenges both experimental spectroscopists and theoreticians [1]. Among the unsolved problems is that of H_3^+ in its electronic triplet state. It has been known for a long time [2–5] that the lowest triplet state, $^3\Sigma_u^+$, possesses three symmetry related shallow minima that might support bound ro-vibrational states. Transitions involving the electronic triplet state might be the source of some of the yet unassigned lines observed in the hydrogen plasmas [6]. Thus, there is a strong demand for accurate calculations of the bound ro-vibrational states to be carried out [6,7]. The only potential energy hypersurface that has been available so far [4] is not of sufficient quality to permit such calculations, as admitted by those authors themselves. In the present paper we present the results of bound state calculations using a new and very accurate local potential energy hypersurface that was obtained by two of the present authors and their collaborators [8].

II. The potential energy hypersurface.—The H_3^+ molecule is linear in its lowest triplet state, with equilibrium bond lengths of $R = 2.4537a_0$. Because of permutational symmetry there are three equivalent structures, separated by tunneling barriers of 2598 cm^{-1} , at $R_1 = R_2 = 5.403a_0$, $R_3 = 1.992a_0$, and equivalent C_{2v} arrangements. The symmetry properties are best described in symmetrized hyperspherical coordinates. We use here the mass-scaled “democratic” coordinates as defined by Whitten and Smith [9] and modified by Johnson [10]. The three internal coordinates are the hyperradius ρ and the two angles θ and ϕ . They are related to the particle distances by

$$R_1 = |\mathbf{r}_2 - \mathbf{r}_3| = \frac{\rho}{\sqrt{3}} [1 + \sin(\theta) \sin(\phi + 4\pi/3)]^{1/2},$$

$$R_2 = |\mathbf{r}_3 - \mathbf{r}_1| = \frac{\rho}{\sqrt{3}} [1 + \sin(\theta) \sin(\phi - 4\pi/3)]^{1/2},$$

$$R_3 = |\mathbf{r}_1 - \mathbf{r}_2| = \frac{\rho}{\sqrt{3}} [1 + \sin(\theta) \sin(\phi)]^{1/2}, \quad (1)$$

with \mathbf{r}_i the position vector of particle i . Thus, for a given value of ρ the geometry of a three-particle arrangement is determined by the two angles θ and ϕ . The equilateral arrangement is at $\theta = 0$, the north pole of the half-sphere, while all collinear arrangements are at $\theta = \pi/2$, the equator. ϕ is the longitudinal angle. A contour plot of the potential energy hypersurface at $\rho = 4.5a_0$ is shown in Fig. 1. We use the stereographic projection $x = 2\rho \tan(\theta/2) \cos(\phi)$ and $y = 2\rho \tan(\theta/2) \sin(\phi)$, with $0 \leq \phi \leq 2\pi$ and $0 \leq \theta \leq \pi/2$. At $x = 0$ and $y = -2\rho$, or $\theta = \pi/2$ and $\phi = \phi_3 = 3\pi/2$, we encounter the singularity $(1, 2) - 3$, i.e., $R_3 = 0$, where the positions of particles 1 and 2 coincide. The two other singularities are located at $\phi = \phi_3 \pm 4\pi/3$. In between are the three symmetry related minima, 3-2-1, 2-1-3, and 1-3-2.

III. Symmetry properties.—The bound ro-vibrational states were calculated using the method of hyperspherical harmonics [11,12]. This method leads directly to a symmetry classification of the calculated bound states according to the three-particle permutation inversion group, $S_3 \times I$ [13]. This group is isomorphic with

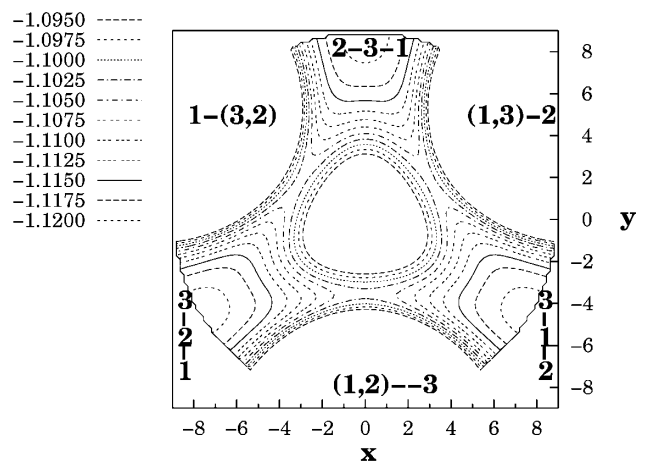


FIG. 1. Contour plot at $\rho = 4.5a_0$, corresponding to the minima. Energy in hartree units.

the molecular symmetry group [13] of tunneling H_3^+ , $D_{3h}(\mathbf{M})$, and has six irreducible representations: A'_1 , A''_1 and A'_2 , A''_2 , which are symmetric and antisymmetric with respect to a permutation of identical particles, and the two twofold degenerate representations E' and E'' . The “prime” states are symmetric with respect to inversion of the spatial coordinate system; the “double prime” states are antisymmetric. Since the hyperspherical harmonics provide a basis of this group, the problem of calculating the bound ro-vibrational states is reduced to six subproblems according to the six irreducible representations, for each value of the total angular momentum [11,12].

We now investigate the symmetry properties of ro-vibrational states of H_3^+ in its lowest electronic triplet state. The vibrational structure can be described in terms of four normal vibrations: the symmetric stretching vibration ν_1 , the twofold degenerate bending vibration ν_2 , and the antisymmetric stretching vibration ν_3 . If the twofold degenerate vibration ν_2 is excited, another quantum number, ℓ , the quantum number of the vibrational angular momentum, exists, which can take the values $\nu_2, \nu_2 - 2, \dots, -\nu_2$. Neglecting the electronic spin, the eigenkets of the ro-vibrational states can be written as

$$|\Psi^\pm\rangle = \frac{1}{\sqrt{2}} |v_1 v_2^{|\ell|} v_3\rangle (|N\ell m\rangle \pm |N - \ell m\rangle), \quad (2)$$

for $\ell \neq 0$ and

$$|\Psi\rangle = \frac{1}{\sqrt{2}} |\Psi^+\rangle \quad (3)$$

for $\ell = 0$. In the above equations N denotes the total angular momentum minus the electronic spin, i.e., $\vec{N} = \vec{J} - \vec{S}$, and m its external projection. The internal projection has to be identical to the vibrational angular momentum ℓ . The states defined in Eq. (2) are eigenstates of the operator for the inversion of the spatial coordinate system, E^* , with characters [13]

$$\chi^{E^*}(|\Psi^\pm\rangle) = \pm(-1)^{N+\ell}. \quad (4)$$

The two states with $\ell \neq 0$ are split in energy, which is known as ℓ -type doubling.

In the group $D_{\infty h}(\text{EM})$, which is the appropriate group as long as tunneling can be neglected, the vibrational states $(v_1, v_2^\ell, v_3) = (0, 0^0, 0)$, $(1, 0^0, 0)$, $(0, 1^1, 0)$, and $(0, 0^0, 1)$ transform as Σ_g^+ , Σ_g^+ , Π_u , and Σ_u^+ . ($D_{\infty h}(\text{EM})$ denotes the extended molecular symmetry group, which is used for the classification of the vibronic states, while $D_{\infty h}(\mathbf{M})$ denotes the molecular symmetry group used for the classification of the ro-vibronic states [13,15].) Since the electronic triplet state has Σ_u^+ symmetry, the vibronic symmetries of the vibrational states are, neglecting the electronic spin, Σ_u^+ , Σ_u^+ , Π_g , and Σ_g^+ . When rotation is taken into account, the vibronic Π_g state is split into ro-vibronic states of Σ_g^+ and Σ_g^- symmetries. The symmetries of the rotational levels of each of the vibronic states in the molecular symmetry group $D_{\infty h}(\mathbf{M})$ can be

obtained using Eq. (4) and the character table of $D_{\infty h}(\mathbf{M})$. Alternatively, they can be read off from Fig. 17-6 of [13], which is related to Fig. 99 of [14]. The result, as well as Herzberg's [14] s/a classification for the symmetry behavior of the ro-vibronic states with respect to permutation of identical nuclei, is presented in Table I. Note that the \pm labels in Herzberg's figure correspond to the superscripts of the ro-vibronic symmetry labels.

The s/a classification is useful for the determination of the statistical weights. In the case of $^1H_3^+$, the three nuclear spins of the protons can be coupled to a totally symmetric quartet state [Σ_g^+ , i.e., (s) symmetry] and two doublet states [$\Sigma_g^+(s)$ and $\Sigma_u^+(a)$]. To yield a total wave function that is antisymmetric with respect to an odd exchange of the protons, the ro-vibronic functions of symmetry (s) can be combined only with the antisymmetric doublet nuclear spin state, resulting in a statistical weight of 2, while the ro-vibronic functions of symmetry (a) can be combined with both the quartet and the symmetric doublet nuclear spin states, thus resulting in a statistical weight of 6.

The potential energy hypersurface shows three equivalent minima which we denote as I , II , and III . The true wave functions must therefore be a superposition of localized functions $|\Psi^\pm\rangle$. Following [16], we write

$$|\Psi_A^\pm\rangle \sim |\Psi_I^\pm\rangle + |\Psi_{II}^\pm\rangle + |\Psi_{III}^\pm\rangle \quad (5)$$

and

$$|\Psi_{E,\xi}^\pm\rangle \sim |\Psi_I^\pm\rangle + \omega |\Psi_{II}^\pm\rangle + \omega^2 |\Psi_{III}^\pm\rangle, \quad (6)$$

$$|\Psi_{E,\eta}^\pm\rangle \sim |\Psi_I^\pm\rangle + \omega^2 |\Psi_{II}^\pm\rangle + \omega |\Psi_{III}^\pm\rangle \quad (7)$$

with $\omega = e^{\frac{2\pi i}{3}}$. The first ket, $|\Psi_A^\pm\rangle$, provides a one-dimensional representation, while the other two, $|\Psi_{E,\xi}^\pm\rangle$ and $|\Psi_{E,\eta}^\pm\rangle$, which are related by complex conjugation, provide the two components of a two-dimensional representation. The classification of the ro-vibronic states of tunneling H_3^+ is with respect to the molecular symmetry group $D_{3h}(\mathbf{M})$ and can be obtained from the classification in $D_{\infty h}(\mathbf{M})$ with the help of the reverse correlation Table VI shown in the appendix. The symmetry classification is presented in Table II. In $D_{3h}(\mathbf{M})$, the quartet nuclear spin function transforms as A'_1 while the two doublet functions become degenerate (E' symmetry). The total wave function has to be antisymmetric with respect to an odd exchange of the protons and hence can be only of symmetry

TABLE I. Symmetry classification of the ro-vibronic states in $D_{\infty h}(\mathbf{M})$. $(0, 1^1, 0)^\pm$ denote the ℓ -type doublets.

(v_1, v_2^ℓ, v_3)	Γ_{rve}	
	N even	N odd
$(0, 0^0, 0)$	$\Sigma_u^+(a)$	$\Sigma_u^-(s)$
$(1, 0^0, 0)$	$\Sigma_u^+(a)$	$\Sigma_u^-(s)$
$(0, 1^1, 0)^+$	$\Sigma_g^-(a)$	$\Sigma_g^+(s)$
$(0, 1^1, 0)^-$	$\Sigma_g^+(s)$	$\Sigma_g^-(a)$
$(0, 0^0, 1)$	$\Sigma_g^+(s)$	$\Sigma_g^-(a)$

TABLE II. Symmetry classification and statistical weights (in parentheses) of the ro-vibronic states of triplet ${}^1\text{H}_3^+$ in $D_{3h}(\text{M})$. $(0, 1^1, 0)_{\pm}$ denote the ℓ -type doublets.

(v_1, v_2^{ℓ}, v_3)	Γ_{rve}	
	N even	N odd
$(0, 0^0, 0)$	$A_2'(4); E'(2)$	$A_1''(0); E''(2)$
$(1, 0^0, 0)$	$A_2'(4); E'(2)$	$A_1''(0); E''(2)$
$(0, 1^1, 0)_+$	$A_2''(4); E''(2)$	$A_1'(0); E'(2)$
$(0, 1^1, 0)_-$	$A_1'(0); E'(2)$	$A_2''(4); E''(2)$
$(0, 0^0, 1)$	$A_1'(0); E'(2)$	$A_2''(4); E''(2)$

A_2' or A_2'' . Therefore, the ro-vibronic states of A_2 symmetry come with the quartet nuclear spin state, while those of E symmetry come with the doublet nuclear spin state. The proton spin statistical weights of the ro-vibronic states are included in Table II in parentheses. The ro-vibronic states of A_1 symmetry have the statistical weight 0.

IV. Topological effects.—Because of symmetry, the potential energy hypersurface of the lowest triplet state, ${}^3\Sigma_u^+$, has a conical intersection with the ${}^3\Sigma_g^+$ state at the D_{3h} configurations, where the two states form a degenerate ${}^3E'$ state. This intersection is very high in energy. The depth of the potential wells of the ${}^3\Sigma_u^+$ state is 2951 cm^{-1} , while the conical intersection is 17992 cm^{-1} above the minima (with the same value of the hyperradius), thus not accessible for the bound ro-vibrational states. To investigate the effect of the conical intersection, we performed explicit calculations using the mixed grid basis method in hyperspherical coordinates suggested by two of the present authors [17]. These calculations were carried out with ordinary cyclic boundary conditions and with modified cyclic boundary conditions to account for the geometric phase. The results obtained for the two sets of calculations are identical to

TABLE III. Ro-vibronic levels, in cm^{-1} , of ${}^1\text{H}_3^+$ in the ${}^3\Sigma_u^+$ electronic state for $N \leq 2$. The dissociation threshold is 1229.1 cm^{-1} above the zero point energy of 1721.6 cm^{-1} .

i	$A_1^{\prime a}$	A_2'	E'	$A_1^{\prime\prime a}$	A_2''	E''
$N = 0$						
0	738.7	0.0	0.0
1	...	973.0	738.8
2	973.1
$N = 1$						
0	666.4	...	666.4	7.2	664.7	7.2
1	981.8	749.0	664.7
2	749.0
3	981.9
$N = 2$						
0	680.6	26.3	26.4	...	685.6	685.6
1	769.4	999.3	680.6
2	769.5
3	999.6

^aMissing levels.

TABLE IV. Ro-vibronic levels, in cm^{-1} , of ${}^1\text{H}_3^+$ in the ${}^3\Sigma_u^+$ electronic state for $N \leq 5$. Tunneling splitting is not resolved.

N	$(0, 0^0, 0)$	$(1, 0^0, 0)$	$(0, 1^1, 0)_+$	$(0, 1^1, 0)_-$	$(0, 0^0, 1)$
0	0.0	973.0	738.7
1	7.2	981.8	666.4	664.7	749.0
2	26.3	999.3	685.6	680.6	769.4
3	54.8	1025.7	713.9	704.6	799.9
4	92.7	1059.9	752.9	736.8	839.9
5	140.1	1103.0	800.9	777.5	890.0

all places. Thus, there is no topological effect present for the bound states, which indicates that the bound states are well localized in the potential minima.

V. Results.—Numerical calculations in the basis of hyperspherical harmonics were performed as described in [12], using nuclear masses. We noticed that for the present system the hyperspherical harmonics expansion converges only slowly, much slower than for the singlet electronic ground state. Typical basis sets consist of about 1500 symmetrized functions [11], contracted to 200 functions at the minimum of the potential. Numerical integration of the set of coupled equations in the hyperradius ρ was then performed within a range of $2.0a_0 \leq \rho \leq 8.0a_0$ and a step size of $\Delta\rho = 0.05a_0$. On the basis of our convergency studies and of occasional cross-checks with the results obtained with the independent method of two of us [17] we believe that the reported numerical data should be exact to about 0.5 cm^{-1} for the given potential energy hypersurface. The complete data for all irreducible representations are presented in Table III for $N \leq 2$. The pattern can be understood as follows: For $N = 0$, which implies $\ell = 0$, the wave functions must have positive parity, according to Eq. (4), and hence must have A_1' , A_2' , or E' symmetry. When passing between even and odd N , the prime states become double prime states and vice versa. As to the states belonging to one-dimensional representations, they change from A_1' to A_2'' or from A_1'' to A_2' , keeping the characters with respect to the operators $(ij)^*$; see Table V in the appendix. Of the $(0, 1^1, 0)$ state, the negative linear combination, Eq. (2), has the same parity as the $\ell = 0$ states, while the positive linear combination has opposite parity.

TABLE V. Correlation table between $D_{3h}(\text{M})$ and $D_{\infty h}(\text{M})$, containing, in addition, the characters with respect to $\chi^{(ij)}$ and $\chi^{(ij)*}$.

$\chi^{(ij)}$	$\chi^{(ij)*}$	$D_{3h}(\text{M})$	$D_{\infty h}(\text{M})$
1	1	A_1'	Σ_g^+
-1	-1	A_2'	Σ_u^+
0	0	E'	$\Sigma_g^+ \oplus \Sigma_u^+$
1	-1	A_1''	Σ_u^-
-1	1	A_2''	Σ_g^-
0	0	E''	$\Sigma_g^- \oplus \Sigma_u^-$

TABLE VI. Reverse correlation table between $D_{\infty h}(M)$ and $D_{3h}(M)$ with the spin statistical weights for ${}^1\text{H}_3^+$ given in parentheses.

$D_{\infty h}(M)$	$D_{3h}(M)$	$D_{\infty h}(M)$	$D_{3h}(M)$
$\Sigma_g^+(2)$	$A_1'(0) \oplus E'(2)$	$\Sigma_u^+(6)$	$A_2'(4) \oplus E'(2)$
$\Sigma_g^-(6)$	$A_2''(4) \oplus E''(2)$	$\Sigma_u^-(2)$	$A_1''(0) \oplus E''(2)$

It can be seen in Table III that the numerical data obtained for any two corresponding tunneling states agree to within 0.3 cm^{-1} , a difference that is not significant. The tunneling splitting is expected to be smaller by several orders of magnitude. For H_3 the tunneling splitting was found to be of the order of 10^{-6} cm^{-1} [18]. In the case of triplet H_3^+ , the top of the tunneling barrier corresponds to a C_{2v} van der Waals complex of H_2^+ with equilibrium bond length and an H atom far away at $5.4a_0$. Even though only 876 cm^{-1} above the zero point energy, this arrangement is not accessible for the linear H_3^+ molecule as it would require strong stretch bend coupling. Since the hyperspherical harmonics expansions converge only slowly, in particular, for E symmetry, and since the tunneling splitting cannot be resolved within the accuracy of the method, numerical data for $N > 2$ were calculated for the one-dimensional representations only. The rotational term values for $N \leq 5$ are presented in Table IV. Even for $N \leq 2$ we use the more accurate numerical data obtained for the one-dimensional representations.

Part of the work was performed during a visit of one of the authors (A.A.) at the Universidade de Coimbra. A.A. gratefully acknowledges financial support by the Deutscher Akademischer Austauschdienst through the INIDA programme (Grant No. 314 inida-dr) and by the Fonds der Chemischen Industrie. Computer time was kindly provided by the RWTH Aachen and the University of Bielefeld. We thank Dr. Dirk Andrae for fruitful discussions.

Appendix.—In Tables V and VI we show the correlation tables between the molecular symmetry groups of localized triplet H_3^+ , $D_{\infty h}(M)$, and of tunneling triplet H_3^+ , $D_{3h}(M)$, which were constructed from the character tables of these groups as given by Bunker and Jensen [13]. In the first table we have included the characters χ of the

representations with respect to permutations of identical particles, (ij) , and permutations combined with inversion of the spatial coordinate system, $(ij)^*$. Note that for the one-dimensional representations $\chi^{(ij)}$ leads to the s/a labels, while $\chi^{(ij)^*}$ characterizes the tunneling states, as explained in the text.

*Corresponding author.

- [1] See papers of a discussion meeting on the subject organized and edited by E. Herbst, S. Miller, T. Oka, and J.K.G. Watson, *Philos. Trans. R. Soc. London A* **358**, 2363 (2000).
- [2] L.J. Schaad and W.V. Hicks, *J. Chem. Phys.* **61**, 1934 (1974).
- [3] R. Ahlrichs, C. Votava, and C. Zirc, *J. Chem. Phys.* **66**, 2771 (1977).
- [4] P.E.S. Wormer and F. de Groot, *J. Chem. Phys.* **90**, 2344 (1989).
- [5] A. Preiskorn, D. Frye, and E. Clementi, *J. Chem. Phys.* **94**, 7204 (1991).
- [6] J. Tennyson, *Rep. Prog. Phys.* **57**, 421 (1995).
- [7] I. McNab, *Adv. Chem. Phys.* **89**, 1 (1995).
- [8] O. Friedrich, A. Alijah, D. Andrae, and J. Hinze (to be published).
- [9] R.C. Whitten and F.T. Smith, *J. Math. Phys. (N.Y.)* **9**, 1103 (1968).
- [10] B.R. Johnson, *J. Chem. Phys.* **79**, 1916 (1983).
- [11] L. Wolniewicz, J. Hinze, and A. Alijah, *J. Chem. Phys.* **99**, 2695 (1993).
- [12] A. Alijah, L. Wolniewicz, and J. Hinze, *Mol. Phys.* **85**, 1125 (1995).
- [13] P.R. Bunker and P. Jensen, *Molecular Symmetry and Spectroscopy* (NRC Press, Ottawa, Ontario, Canada, 1998), 2nd ed.
- [14] G. Herzberg, *Molecular Spectra and Molecular Structure II: Infrared and Raman Spectra of Polyatomic Molecules* (Krieger Publishing Co., Malabar, FL, 1991), reprint edition.
- [15] P.R. Bunker and D. Papousek, *J. Mol. Spectrosc.* **32**, 419 (1969).
- [16] I.N. Levine, *Molecular Spectroscopy* (Wiley, New York, 1975).
- [17] A.J.C. Varandas and Z.R. Xu, *Int. J. Quantum Chem.* **75**, 89 (1999).
- [18] G.C. Hancock, C.A. Mead, D.G. Truhlar, and A.J.C. Varandas, *J. Chem. Phys.* **91**, 3492 (1989).